Available online at www.sciencedirect.com
SCIENCE DIRECT®
International Journal of Heat and Mass Transfer 49 (2006) 1452–1461
International Journal of HEAT and MASS TRANSFER
www.elsevier.com/locate/ijhmt

Convective heat transfer in porous channels with 90-deg turned flow

Sheng-Chung Tzeng [a,*], Tzer-Ming Jeng [b]

[a] Department of Mechanical Engineering, Chienkuo Technology University, No. 1, Chieh Shou N Rd., Chang Hua 500, Taiwan, ROC
[b] Department of Mechanical Engineering, Air Force Institute of Technology, GangShan 820, Taiwan, ROC

Received 29 July 2005; received in revised form 10 September 2005
Available online 22 November 2005

Abstract

This study experimentally investigated the convective heat transfer and pressure drop in porous channels with 90-deg turned flow. Aluminum foams with a porosity of 0.93 were used. The size of the aluminum foams was fixed. Variable parameters were the ratio of the entry width to the porous sink height (W_j/H), the pore density of the aluminum foam (PPI, pore per inch) and the Reynolds number (Re). Experimental results reveal that the wall temperature was maximal at the corner under perpendicular flow entry. It fell along the channel axis until x/H was about 1.0, finally approaching a constant value. Parametric studies indicate that increasing Re increased the average Nusselt number ($\overline{Nu}$) and the effects of W_j/H and PPI on $\overline{Nu}$ were negligible. The friction factor (C_f) generally declined as Re increased, PPI decreased or W_j/H increased. Besides, increasing W_j/H or reducing PPI slightly increased $\overline{Nu}$ at a given pumping power. Additionally, the heat transfer and pressure drop in porous channels with straight flow were also measured for comparison.

Keywords: Heat transfer; Pressure drop; Porous channels; 90-deg turned flow

1. Introduction

A porous metallic material can be treated as a compact heat sink in electronic cooling applications. Such a porous metallic material has two advantages: first, the porous material has a much larger dissipation area than does a conventional finned sink, promoting heat convection. Second, the irregular structure of the porous materials, at sufficiently large velocities, is responsible for the irregular motion of the fluid flow. The flow separates around the individual beads or fibers, mixing the fluid more effectively. Therefore, the thermal dispersion conductivity greatly exceeds the fluid thermal conductivity.

The measurement of heat transfer in porous media has been studied extensively. Hunt and Tien [1] experimentally measured forced convection in channels filled with various porous foam materials. Their results demonstrated that the dispersive transport increases with flow rate and permeability. Chou et al. [2] experimentally investigated forced convection in horizontal square channels through packed spheres. They found that the values of the fully-developed Nusselt number are influenced mainly by the channeling effect when the Peclet number is small, but the thermal dispersion effect becomes dominant when the Peclet number is high. Hwang and Chao [3] measured heat transfer through sintered bronze bead porous channels. Their measurement covered the data in both thermal entrance and thermally fully developed regions. They also introduced a wall function to model the transverse thermal dispersion process for the wall effect on the lateral mixing of fluid. Calmidi and Mahajan [4] experimentally and numerically examined forced convection in highly porous aluminum foams, using air as a cooling fluid. The empirical constants, such as the solid-to-fluid heat transfer coefficient and the thermal dispersion conductivity, were determined by matching the numerical results with their experimental data and those in the open literature. Kim et al. [5] experimentally explored the effect of aluminum foam on the flow and convective heat transfer in an asymmetrically heated channel. They provided a correlation of the friction factor and the

* Corresponding author. Tel.: +886 4 7111111x3132; fax: +886 4 7357193.
E-mail addresses: tsc@ctu.edu.tw, tsc33@ms32.hinet.net (S.-C. Tzeng).

0017-9310/$ - see front matter © 2005 Elsevier Ltd. All rights reserved.
doi:10.1016/j.ijheatmasstransfer.2005.09.024

Nomenclature

C_f	friction factor, $(p_i - p_e)/(0.5\rho_f U_e^2)$
Da	Darcy number, K/H^2
F	inertial coefficient
H	height of the porous medium (m)
H_b	height of the spreader (m)
h_v	volumetric heat transfer coefficient (W/m^3 °C)
K	permeability (m^2)
k	thermal conductivity (W/m/°C)
L	length of the porous medium (m)
$\overline{Nu}$	average Nusselt number, Eq. (3)
Nu_{fs}	fluid-to-solid Nusselt number, $h_v H^2/k_f$
p	pressure (Pa)
PPI	pore density of the metal foam, pore per inch
q_c	convective heat flux (W/m^2)
q_k	conductive heat loss (W/m^2)
q_r	radiative heat loss (W/m^2)
q_t	total heat flux generated by the thermofoil heater (W/m^2)
Re	Reynolds number, $\rho_f U_e H/\mu$
s	spacing between thermocouples
T	temperature (°C)
U	average fluid velocity (m/s)
W	width of the porous medium (m)
W_j	width of the perpendicular flow entry
x	axial coordinate (m)

Greek symbols

ε	porosity
μ	viscosity (kg/m/s)
θ	dimensionless temperature, $(T - T_i)/(q_c H/k_f)$
ρ	density (kg/m^3)

Superscript

*	effective

Subscripts

e	channel exit
f	fluid
i	channel inlet
s	solid matrix
w	channel wall

average Nusselt number to be a guide in practical applications. Boomsma et al. [6] experimentally studied pressure drops and wall Nusselt numbers in compressed metal foams. Fu et al. [7] and Leong and Jin [8,9] experimentally investigated the heat transfer associated with steady and oscillating flows in a channel filled with aluminum foam or copper foam. The effects of the dimensionless amplitude of displacement and dimensionless frequency of oscillating flow were considered. They reported the porous channel heat sink subjected to oscillating flow can be regarded as an effective method for cooling high-speed electronic devices. Bhattacharya and Mahajan [10] experimental explored the forced convective heat transfer in novel finned metal foam heat sinks. Their results showed that heat transfer is significantly enhanced when fins are incorporated in metal foam. The heat transfer coefficient increases with increase in the number of fins until adding more fins retards heat transfer due to interference of thermal boundary layers. Ko and Anand [11] carried out a series of measurements to investigate the average heat transfer coefficients in uniformly heated rectangular channel with wall mounted porous baffles. In their experiments, the use of porous baffles resulted in heat transfer enhancement as high as 300% compared to heat transfer in straight channel with no baffles. Jiang et al. [12] experimentally examined heat transfer by forced convection in sintered porous channels. They indicated that the heat transfer enhancement due to the sintered porous media intensifies sharply with increasing flow rate. However, the effect of particle diameter on the convective heat transfer in the sintered porous media is not great. The works cited herein provide insights into the heat transfer by porous metallic materials. The results of these studies reveal that a porous material can be used as an effective heat sink, possibly providing an effective method for cooling circuit boards on which heat-generating electronic components are mounted.

All of the aforementioned investigations had a typical inlet flow direction that was parallel to the channel axis. However, this is commonly not a realistic inlet configuration for heat exchangers, in which coolant flow generally turns through a serpentine-shaped passage before entering the heat sinks. Accordingly, this work focuses on a different issue, considering the case in which flow enters the porous heat sink immediately following a 90-deg turn. Few studies have addressed this issue. Chyu et al. [13] and Hwang and Lui [14] measured the heat transfer coefficients at the surface of fins and the uncovered endwall surface in channels with pin-fin arrays and 90-deg turned flow, respectively. Fu and Huang [15] numerically elucidated the promotion of forced convection by a slot jet that impinges on a non-sintered porous block mounted on an isothermally heated wall, in which the jet flow turned toward the transverse direction of the jet near the stagnation line. However, experiments have not yet been conducted to determine the heat transfer performance in porous metallic foam channels with 90-deg turned flow. The streamline pattern in a 90-deg turned channel is more complicated than that in a straight channel. Fig. 1 presents the numerical result of a typical streamline pattern associated with laminar flow turned through 90-deg. Such a flow field normally includes two vortices, which is consistent with the combination of the flow characteristics of step flow and confined jet flow.

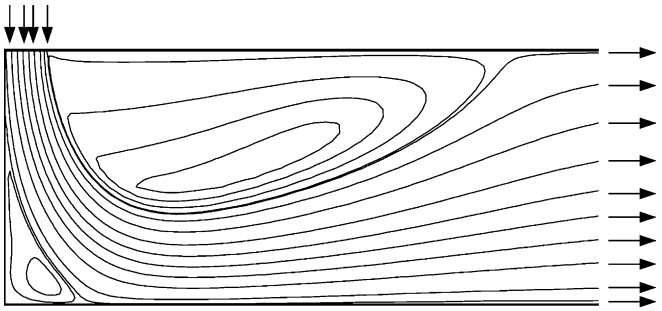

Fig. 1. Typical streamline pattern for the 90-deg turned flow.

One is present next to the perpendicular flow entry, promoting the transfer of heat on the bottom wall; the other is generated at the corner under the perpendicular flow entry, reducing the transfer of heat. These results motivate this work.

This investigation addressed the convective heat transfer and pressure drops in porous channels with 90-deg turned flow. Aluminum foams with a porosity of 0.93 were employed. The coolant was air. The size of the aluminum foams was fixed. Variable parameters were the ratio of the entry width to the porous sink height (W_j/H), the pore density of the aluminum foam (PPI, pore per inch), and the Reynolds number (Re). The heat transfer and pressure drop in porous channels with straight flow were also measured for comparison. Additionally, the relationships of both the average Nusselt number ($\overline{Nu}$) and the friction factor (C_f) with W_j/H, PPI and Re were obtained, based on the present experimental data.

2. Experimental setup

2.1. Test section and apparatus

The experimental system, presented in Fig. 2, comprises three parts—a wind tunnel, a porous medium test section and a data acquisition system. The wind tunnel is made of 10 mm-thick Plexiglas plates. The main flow of air was supplied using a blowing machine, and the flow rate was controlled using a frequency inverter. After it passes through a straightening section, the flowing air enters the test channel from the perpendicular entries of various widths or the straight entry of fixed height. The test channel made of 40 mm-thick Bakelite plates has a rectangular cross section of 60×25.4 mm filled with 60 mm-long aluminum (alloy 6101-T6) foams with a thermal conductivity of 218 W/m °C. A thermofoil heater was attached to the inner surface of the bottom wall of the test channel. The other walls of the channel were insulated. Aluminum foams (as shown in Fig. 3) are typically available in high porosities and have an open-celled structure. Table 1 provides the porous characteristics of the aluminum foams, such as the permeability (K), the inertial coefficient (C_F), the effective solid conductivity (k_s^*), etc. The K and C_F values were determined by the method reported by Hunt and Tien [1]. The value of k_s^* was measured by performing a number of one-dimensional conduction heat transfer experiments (the test method can be found in Ref. [16]). The aluminum foams with porosities of 0.93 have pore densities of 10 and 40 PPI (pores per inch). These aluminum foams were brazed onto 3 mm-thick aluminum spreaders. Eight 36-gauge T-type thermocouples were fixed to the bottom skin of the spreader along the channel axis, as displayed in Fig. 4. Seven other thermocouples were used to monitor the ambient temperature, the air temperature at the channel inlet and the air temperature at the channel exit. A total of 15 thermocouples were connected to the data logger. The system was assumed to be in a steady state when the temperature did not vary by over 0.2 °C during an interval of 15 min. An anemometer was installed in the rear section after the test section to measure the speed of the airflow, and a pressure transmitter was utilized to measure the pressure drop associated with the flow of air through the test section.

2.2. Data reduction and uncertainty analysis

The measured fluid velocities, temperatures and pressure drops were used to determine the dimensionless wall temperatures, the Reynolds numbers, the average Nusselt numbers and the friction factors, using

$$\theta_w = \frac{T_w - T_i}{q_c H/k_f} \tag{1}$$

$$Re = \frac{\rho_f U_e H}{\mu} \tag{2}$$

$$\overline{Nu} = \frac{hL}{k_f} = \left(\sum_{i=1}^{8} \frac{s}{\theta_{w,i}} \frac{L}{H} \right) \Big/ L \tag{3}$$

$$C_f = \frac{p_i - p_e}{0.5 \rho_f U_e^2} \tag{4}$$

where T_w is the temperature measured at the bottom skin of the aluminum foam heat sink; T_i is the air temperature at the channel inlet; H is the height of aluminum foam; q_c represents the convective heat flux; U_e represents the average air velocity at the channel exit; s is the spacing between thermocouples; L is the length of aluminum foam, and p_i and p_e are the static pressures at the channel inlet and exit, respectively. The total heat flux (q_t) generated by the thermofoil heater may be transformed into three heat-transfer modes in the steady-state experiment to evaluate the convective heat flux dissipated from the heated surface, as determined by the conservation of energy. These modes are, (1) radiative heat loss, q_r; (2) conductive heat loss, q_k, and (3) convective heat dissipated from the heated surface, q_c. Accordingly

$$q_c = q_t - q_r - q_k \tag{5}$$

This energy-balance equation determines the net convective heat flux (q_c) from the heated surface to the flowing air in the channel. The total heat flux (q_t) is V^2/R. Herein, V is

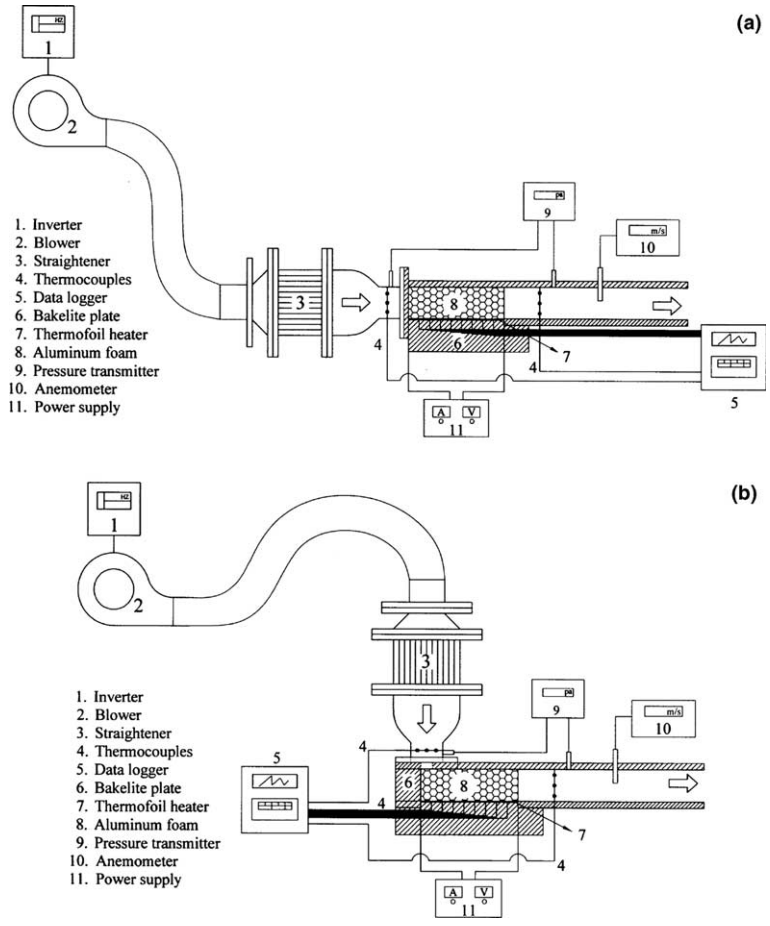

Fig. 2. Experimental apparatus. (a) Flow channel with 90-deg turned flow and (b) flow channel with straight flow.

the output voltage of the DC power supply and R is the resistance of the thermofoil heater. The radiative heat loss (q_r) from the inlet and exit surfaces of aluminum foam to its surroundings, is obtained using thermally diffusive gray-body networks. The maximum radiative heat loss is under 2.1% of the total input heat flux herein. The conductive heat loss (q_k) to the insulated Bakelite is estimated using a two-dimensional conduction models. The q_k values vary from 0.2% to 3.2% of the total input heat flux in the experiments. Hence, the convective heat dissipated from the heated surface (q_c) can be determined, and the dimensionless wall temperatures (θ_w) and the average Nusselt numbers ($\overline{Nu}$) finally calculated.

The standard single-sample uncertainty analysis, as recommended by Kline and Mcclintock [17] and Moffat [18], was performed. Data supplied by the manufacturer of the instrumentation stated that the measurement of flow velocity and pressure drop have a 1% error. The uncertainty in the measured temperature was ±0.2 °C. The experimental uncertainty in the convective heat flux (q_c) was estimated to be 2.4%. The experimental data herein reveal that the uncertainties in the Reynolds number, the friction factor and the average Nusselt number were 1.5%, 2.2% and 7.1%, respectively.

3. Results and discussion

The convective heat transfer, $\overline{Nu}$, in the porous channels with 90-deg turned air flow and isoflux heating on the bottom wall (Fig. 4), is a function of several dimensionless parameters and is given by

$$\overline{Nu} = \overline{Nu}\left(\frac{L}{H}, \frac{W}{H}, \frac{W_j}{H}, Da, Nu_{fs}, Re\right) \tag{6}$$

where ($W \times H \times L$) is the size of the aluminum foam heat sink and is constant herein; W_j is the width of the perpendicular flow entry; Da ($\equiv K/H^2$, where K is the permeability) is the Darcy number; Nu_{fs} ($\equiv h_v H^2/k_f$, where h_v is the volumetric heat transfer coefficient) is the fluid-to-solid Nusselt number, and Re is the Reynolds number. Therefore, Eq. (6) can be reduced to be

$$\overline{Nu} = \overline{Nu}\left(\frac{W_j}{H}, Da, Nu_{fs}, Re\right) \tag{7}$$

Herein, W_j, PPI and the mass flow rate are variable. When PPI and the mass flow rate are fixed, increasing W_j enlarges the perpendicular-flow region (as presented in Fig. 1), reducing the flow velocity during perpendicular flow entry. Accordingly, in that local region, Nu_{fs} also falls.

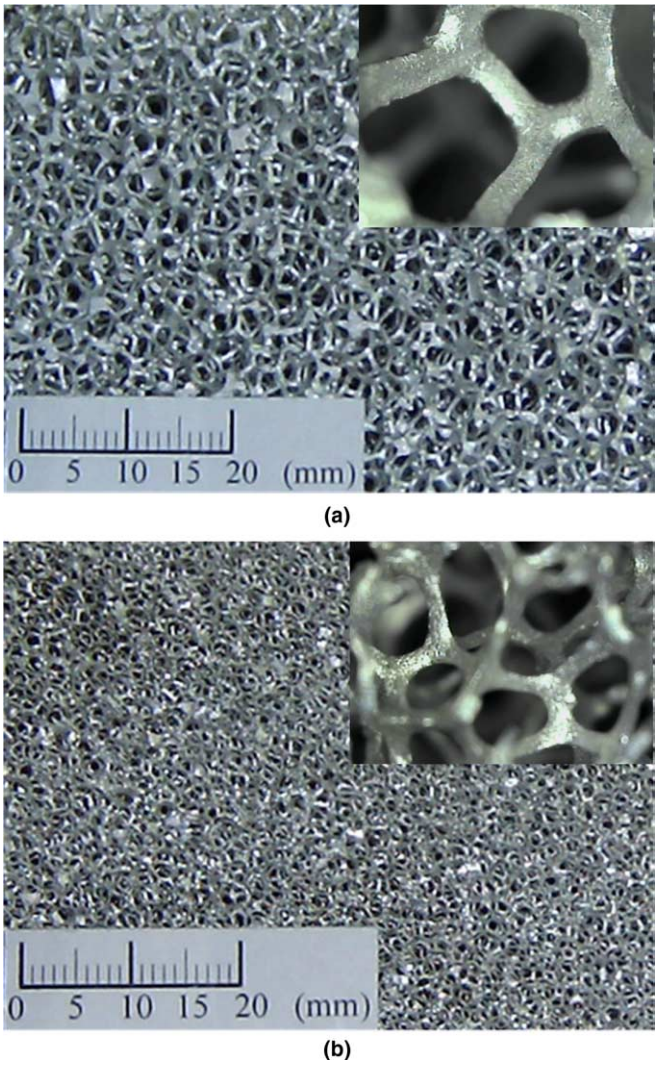

Fig. 3. Pictures of aluminum foam samples with various PPI values. (a) $\varepsilon = 0.93/10$ PPI and (b) $\varepsilon = 0.93/40$ PPI.

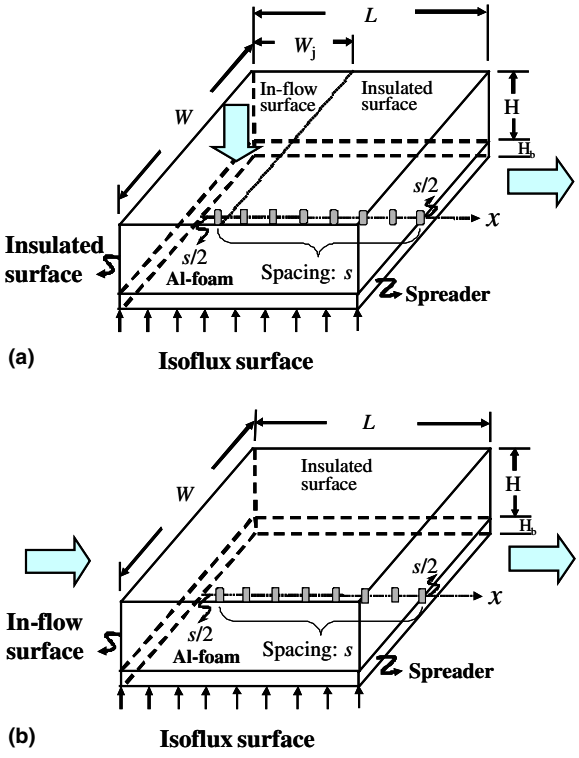

Fig. 4. Test specimen and positions of thermocouples. (a) 90-deg turn flow and (b) straight flow.

Moreover, the coolant with a small perpendicular flow velocity cannot easily penetrate the aluminum foam to near the heated surface. Hence, the heat transferred by the porous heat sink may drop as W_j increases. When W_j and the mass flow rate are constants, increasing PPI reduces Da and increases Nu_{fs}. A small Da of a porous system indicates a large flow resistance, such that less air reaches the heated surface. This weakens the cooling capacity of the porous heat sink. However, the increasing Nu_{fs} promotes the convective heat transfer. Therefore, the overall effect of PPI on the thermal performance of the porous heat sink is governed by these two contrary effects. Finally, W_j and the PPI value are invariable, so a large Re enhances convective heat transfer (Nu_{fs}) and facilitates the passing of the air through the aluminum foam to cooling the heated surface, suggesting that the heat transfer rate is favorable. In this investigation, W_j/H varies from 0.164 to 0.972; $PPIs$ are 10 and 40, and Re varies from 1376 to 23,619. A series of experiments are conducted to elucidate the effects of W_j/H, PPI and Re on the convective heat transfer in a porous channel with 90-deg turned flow.

The experimental data concerning the heat transfer characteristics of a porous channel with 90-deg turned flow are lacking, so the validity of the experiments conducted herein is established by comparing the data on the porous system with straight flow, with data obtained by others. Fig. 5 presents the results of the comparison. The thermal characteristic, $\overline{Nu}/L$, is used to compare the data herein with those that pertain to aluminum foams of various lengths, obtained by Calmidi and Mahajan [4] and Kim et al. [5]. This figure reveals that all of the coefficients of proportionality, n, between the Reynolds number (Re^n) and $\overline{Nu}$ were similar, at $n = 0.4$–0.6. The $\overline{Nu}$ values herein were around 14% higher than those measured by Calmidi and Mahajan [4] because shorter aluminum foams were used herein. The local Nusselt number is maximal at the

Table 1
Characteristics of aluminum foam samples used herein

No. ($W \times H \times L$ mm)	ε	PPI	F	K ($\times 10^8$ m^2)	k^* (W/m °C)
1 ($60 \times 25.4 \times 60$)	0.93	10	0.0476	23.4	5.23
2 ($60 \times 25.4 \times 60$)	0.93	40	0.0460	7.18	5.37

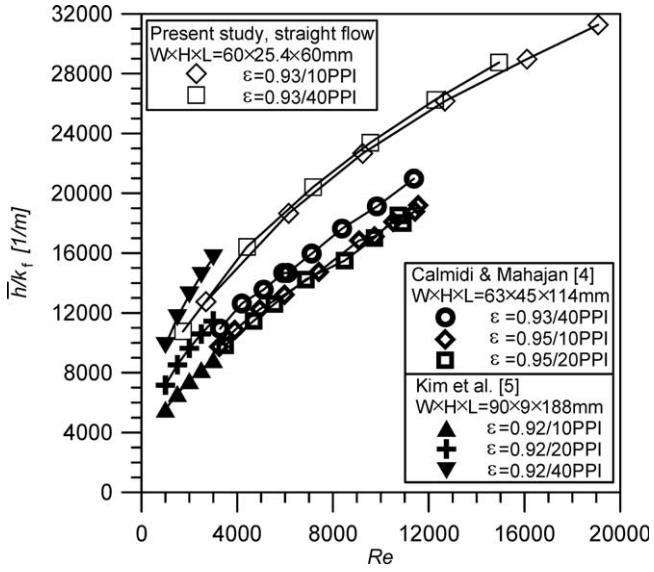

Fig. 5. Comparison with others' data for straight flow configuration.

channel inlet and slowly decreases in the direction of the flow, so $\overline{Nu}$ for the system with shorter aluminum foams exceed that with longer foams. Although the data obtained by Kim et al. [5] show that $\overline{Nu}/L$ increased with PPI values, the data of Calmidi and Mahajan [4] indicate that the effect of PPI on $\overline{Nu}/L$ was insignificant, which finding was consistent with the results herein. The fluid stream and the porous solid matrix are inferred to be in local thermal equilibrium (LTE) over the range of Reynolds numbers considered by Calmidi and Mahajan [4] and this work. When LTE is reached, the thermal characteristics depend mainly on k_s^*. Additionally, aluminum foams with the same porosity and various PPI values have similar k_s^* values, suggesting similar heat transfer behaviors at LTE. Therefore, the comparison with others' experimental data demonstrates that the measurements herein are reasonable.

Fig. 6 shows the dimensionless wall temperatures (θ_w) along the channel axis for a flow that turns through 90-deg with various W_j/H, PPI and Re. In this investigation, the frequency of the inverter was varied to control the air flow rate. Six frequencies, 10, 20, 30, 40, 50 and 60 Hz, were

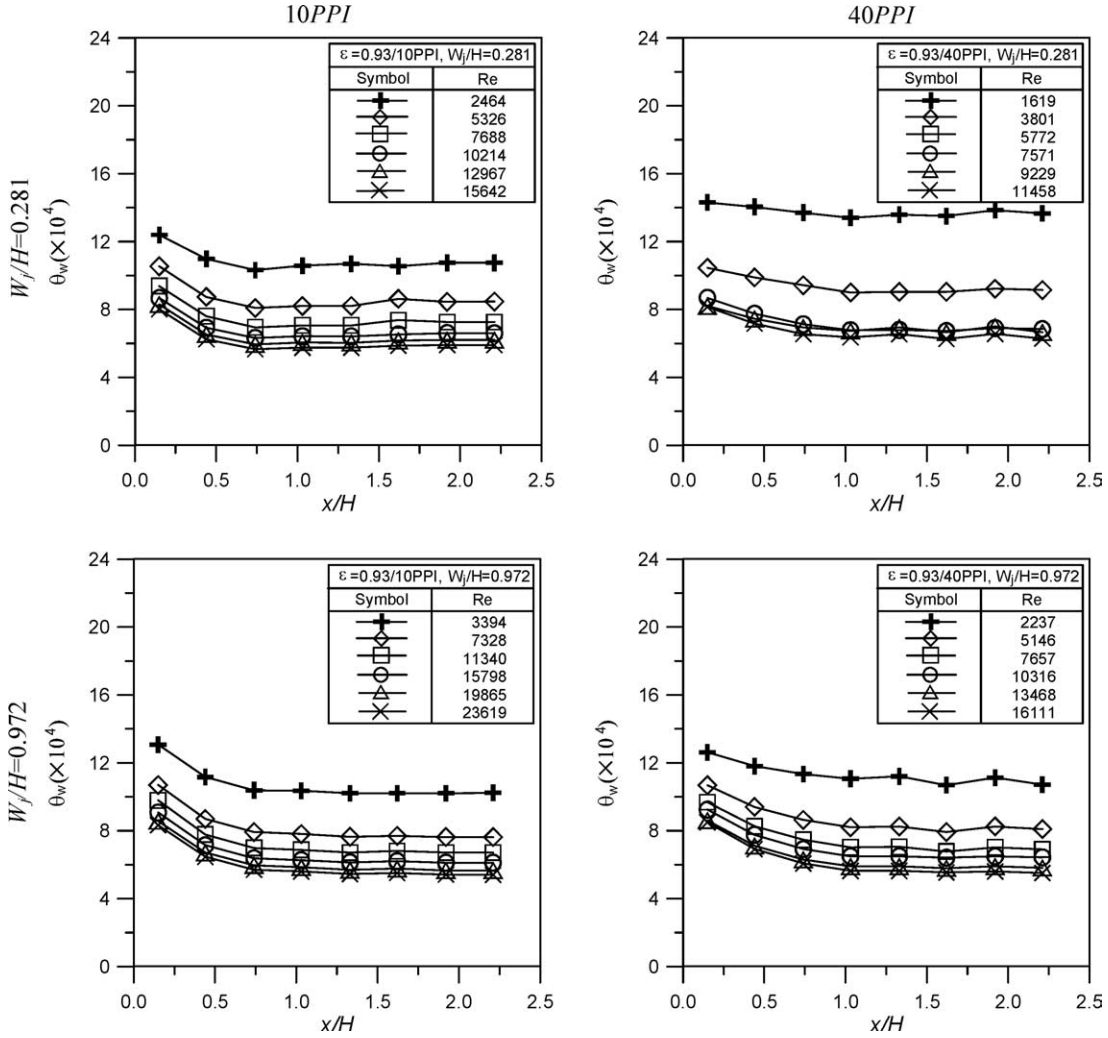

Fig. 6. Dimensionless wall temperatures along the channel axis for 90-deg turned flow with various W_j/H, PPI and Re.

used. The systems with various W_j/H and PPI yield various Re values at a given frequency. Fig. 6 reveals that all of the θ_w distributions were similar. The θ_w at the corner under the perpendicular flow entry was maximal, and declined along the channel axis, until x/H was around 1.0. It finally approached a constant value. This finding agrees with the earlier statement concerning the typical streamline pattern associated with flow that turns through 90-deg. The typical streamline pattern for flow that turns through 90-deg reveals a vortex at the corner under the perpendicular flow entry. This vortex stops convective heat transfer and results in a locally high θ_w. Fig. 7 plots the dimensionless wall temperatures (θ_w) along the channel axis when the flow is straight (such that the flow direction is parallel to the channel axis) for various Re and PPI. The θ_w distribution when the flow is straight differed significantly from that when the flow was turned through 90-deg. For straight flow, θ_w was minimal at the channel inlet and slowly increased along the channel axis until the channel exit. Accordingly, the straight flow configuration is appropriate in a system with a large heat flux at the channel inlet. In contrast, the configuration in which the flow turns through 90-deg should not be applied in the system with a large heat flux at the channel inlet.

Fig. 8 displays the average Nusselt number ($\overline{Nu}$) as a function of the Reynolds number for various PPI and W_j/H. The experimental data in Fig. 8(a) show that increasing Re increased $\overline{Nu}$ in the configuration in which

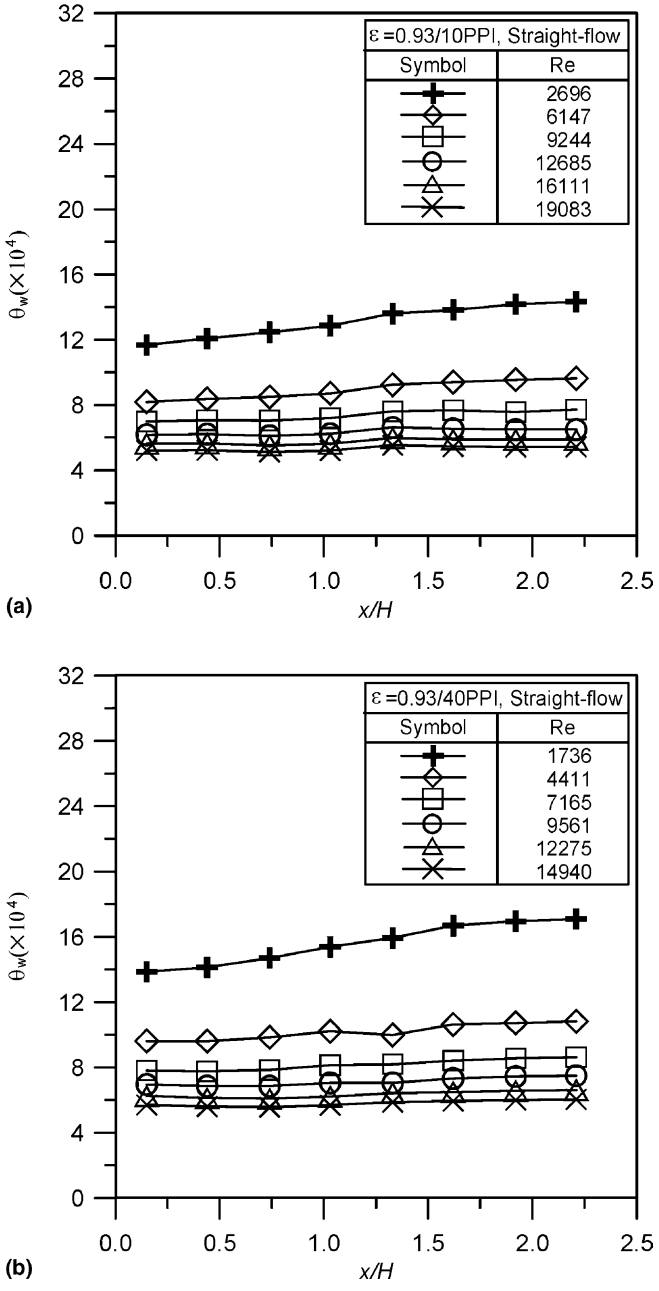

Fig. 7. Dimensionless wall temperatures along the channel axis for straight flow with various PPI and Re. (a) 10 PPI and (b) 40 PPI.

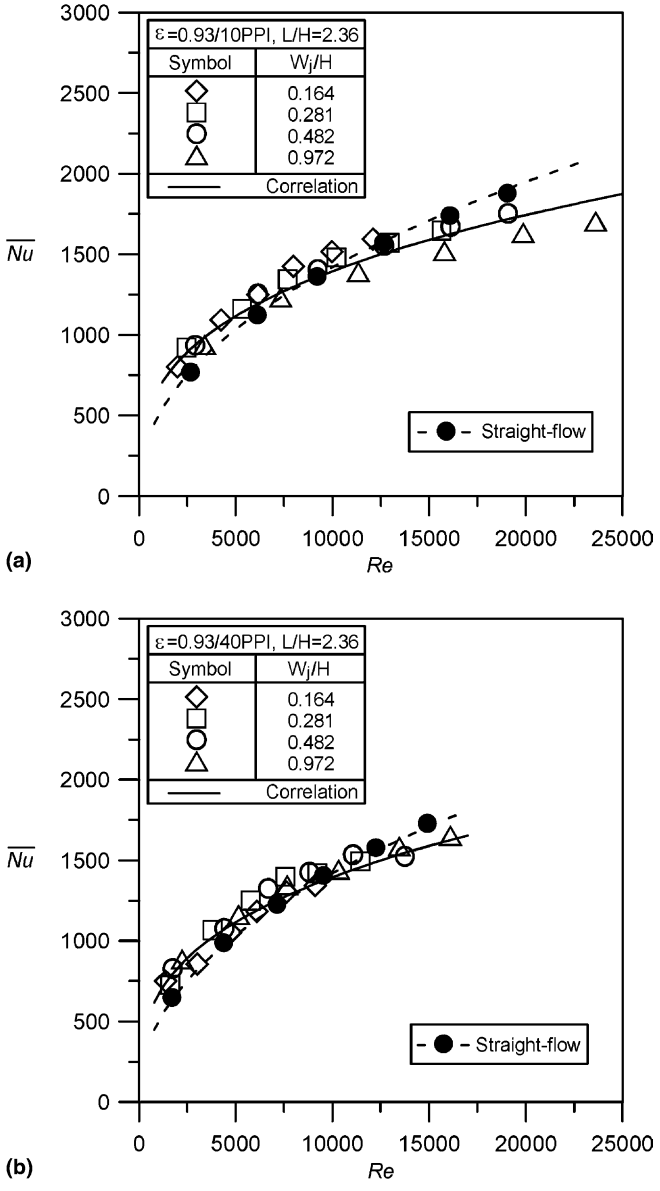

Fig. 8. Average Nusselt number as a function of Reynolds number for various W_j/H and PPI. (a) 10 PPI and (b) 40 PPI.

the flow turned through 90-deg in aluminum foam with $\varepsilon = 0.93/10$ PPI. This fact is consistent with forced convection. W_j/H increased as $\overline{Nu}$ fell, which relationship also agrees with the above comments on the effect of W_j/H on the $\overline{Nu}$. However, based on the data herein, the effect of W_j/H on $\overline{Nu}$ was small. However, Fig. 7(b) demonstrates that $\overline{Nu}$ increased with Re in the configuration in which the flow turned through 90-deg in aluminum foam with $\varepsilon = 0.93/40$ PPI. Additionally, the dependence of $\overline{Nu}$ of 10-PPI aluminum foam on the Reynolds number (Re^n) was similar to that for 40-PPI aluminum foam, suggesting that the effect of the PPI value on $\overline{Nu}$ was negligible. As for the system with aluminum foam for which $\varepsilon = 0.93/10$ PPI, the effect of the W_j/H on $\overline{Nu}$ was also insignificant. Fig. 8 also plots the data concerning the straight flow configuration. For the range of Reynolds numbers considered herein, $\overline{Nu}$ in the straight flow configuration generally neared the values obtained in the configuration in which the flow turned through 90-deg. However, $\overline{Nu}$ in the straight flow configuration depended on the Reynolds number (Re^n) most strongly than in the configuration in which the flow turned through 90-deg. When $Re < 1000$, $\overline{Nu}$ in the configuration in which the flow turned through 90-deg slightly exceeded that in the straight flow configuration. When $Re > 1000$, $\overline{Nu}$ associated with the straight flow configuration slightly exceeded $\overline{Nu}$ in the configuration in which the flow turned through 90-deg. According to the experimental data, the relationship between $\overline{Nu}$ and Re is given by,

$$\overline{Nu} = 71.88Re^{0.322} \quad \text{for flow that turns through 90-deg} \tag{8}$$

$$\overline{Nu} = 21.10Re^{0.457} \quad \text{for straight flow} \tag{9}$$

The average deviation in Eqs. (8) and (9) was 5.42%. The range of application of Eq. (8) is $W_j/H = 0.164$–0.972 and $Re = 1376$–$23{,}619$, for $\varepsilon = 0.93/10$, 40 PPI aluminum foams and $L/H = 2.36$. That of Eq. (9) is $Re = 1736$–$19{,}083$ for $\varepsilon = 0.93/10$, 40 PPI aluminum foams and $L/H = 2.36$.

Fig. 9 displays effects of W_j/H, PPI and Re on the friction factor (C_f) in an aluminum foam channel in which flow turns through 90-deg. The experimental data indicate that the friction factor generally dropped as the Reynolds number increased. However, an unusual phenomenon of C_f increasing with Re for both $W_j/H = 0.164$ and 0.281 and $\varepsilon = 0.93/10$PPI foam were depicted in Fig. 9(a). It may be induced by the onset of the big vortex next to the perpendicular flow entry. A big vortex next to the perpendicular flow entry is expected for the porous system with a large inlet velocity and high permeability. Therefore, the effective flowing channel located between the vortex zone and the bottom surface becomes narrow, suggesting an additional pressure drop due to the acceleration effect of fluid flow. Besides, at the given W_j/H and Re, the friction factor of the system with 40 PPI exceeds that with 10 PPI, because the 40-PPI aluminum foam (Fig. 3) is made of many very

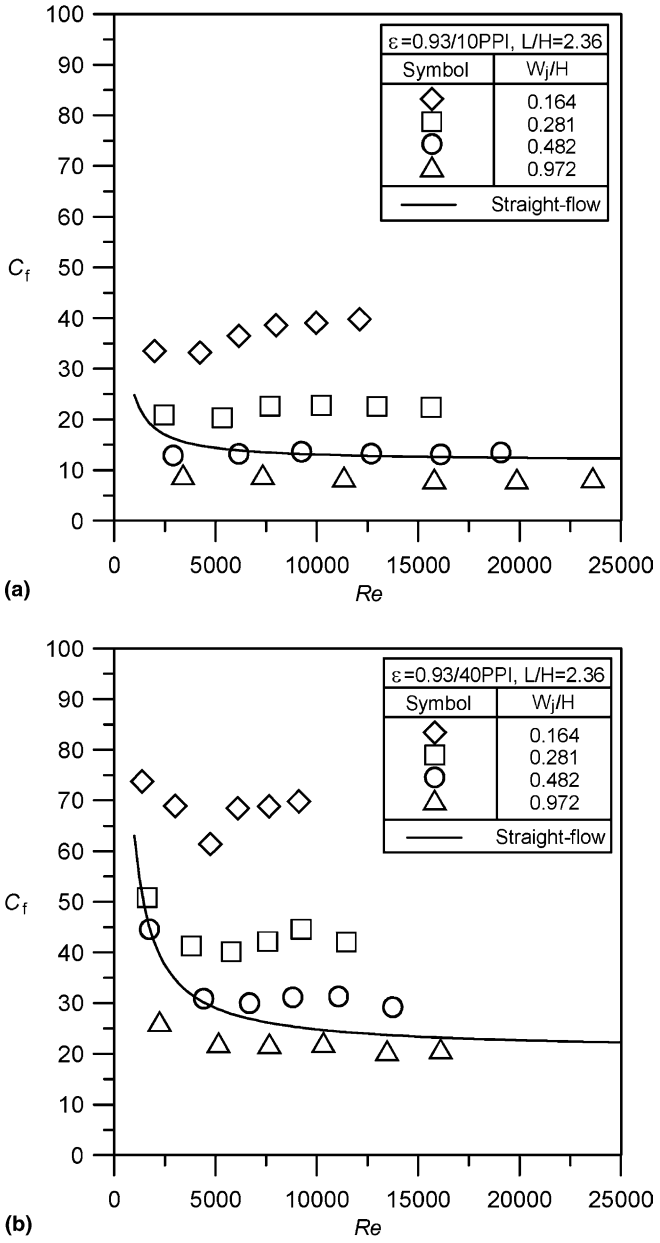

Fig. 9. Friction factor as a function of Reynolds number for various W_j/H and PPI. (a) 10 PPI and (b) 40 PPI.

fine open-cells, which cause a high flow resistance. Additionally, the friction factor increased as W_j/H decreased when the PPI and Re were specified. This relationship can be explained as follows. The pressure drop in a porous channel in which flow turns through 90-deg has two causes. One is the 90-deg turn; the other is the porous medium. Fig. 10 plots the friction factor as a Reynolds number, for the empty channels in which flow turns through 90-deg with various W_j/H. The figure shows that the pressure drops caused by the 90-deg turn of the flow increase as W_j/H decreases. Moreover, the pressure drops in the perpendicular flow regions of the porous channels may fall as W_j/H increases, because at a particular Re, a large W_j/H is responsible for a small perpendicular flow velocity. The

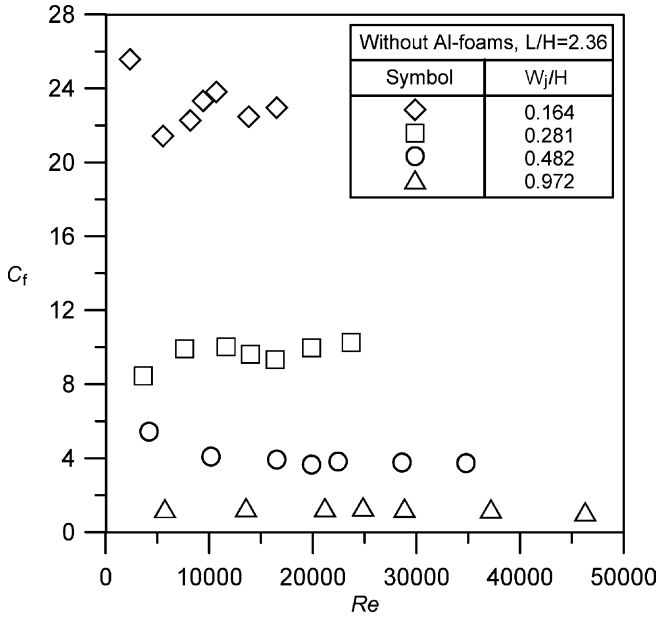

Fig. 10. Friction factor as a function of Reynolds number for the system without Al-foams.

friction factor of the porous channel with straight flow is expressed in the following form:

$$C_f = \frac{2L}{H}\left(\frac{1}{ReDa} + \frac{F}{\sqrt{Da}}\right) \quad (10)$$

where Da ($\equiv K/H^2$, where K is the permeability) is the Darcy number and F is the inertial coefficient. Fig. 9 reveals that the friction factor of the porous channel with straight flow is generally below that of the porous channel with 90-deg turned flow.

Attention is now turned to the pumping power constraint. For systems with various W_j/H and PPI, a fixed pumping power can yield various rates of flow of the air used to cool the heated surface. A dimensionless parameter, C_fRe^3, was introduced as the pumping power. Fig. 11 plots the average Nusselt number ($\overline{Nu}$) against C_fRe^3. The $\overline{Nu}$ increased with C_fRe^3 for systems with various W_j/H and PPI. The data depict that the $\overline{Nu}$ in the configuration in which the flow turned through 90-deg slightly exceeded that in the straight flow configuration when $C_fRe^3 < 1000$. When $C_fRe^3 > 1000$, $\overline{Nu}$ associated with the straight flow configuration slightly exceeded $\overline{Nu}$ in the configuration in which the flow turned through 90-deg. For the configuration in which the flow turns through 90-deg, increasing W_j/H slightly increased $\overline{Nu}$ for a particular C_fRe^3. Additionally, the $\overline{Nu}$ of the system with aluminum foam for which $\varepsilon = 0.93/10$ PPI slightly exceeded that with aluminum foam for which $\varepsilon = 0.93/40$ PPI.

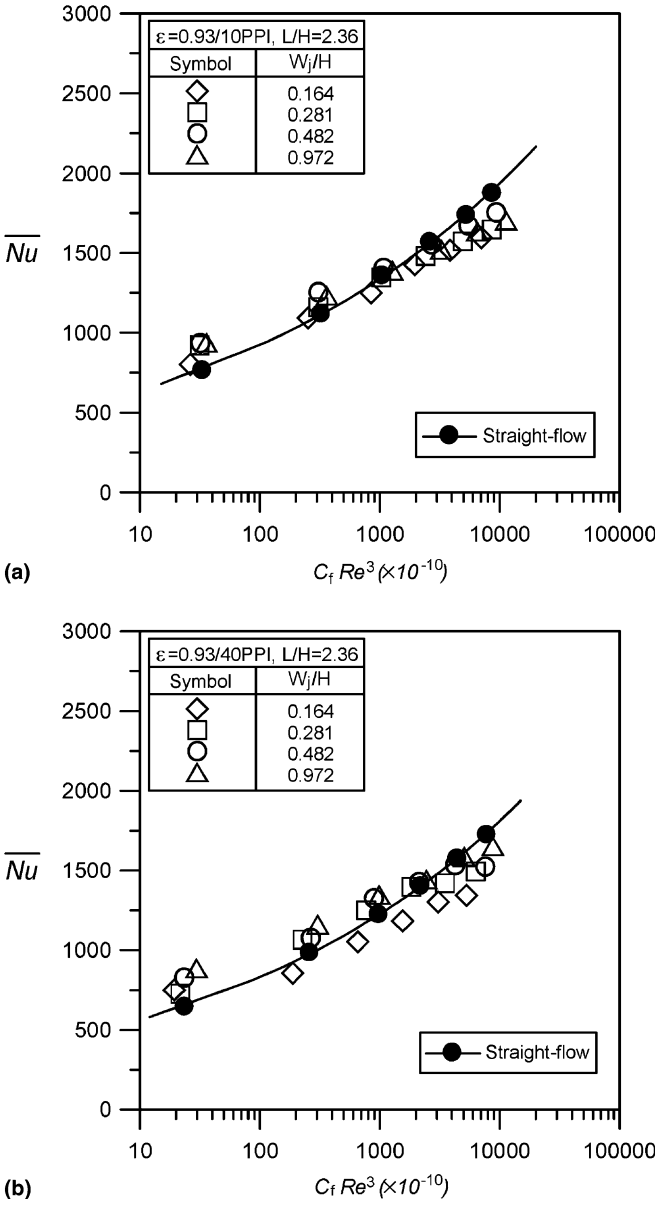

Fig. 11. Average Nusselt number as a function of $C_f\,Re^3$ for various PPI and W_j/H (a) 10PPI (b) 40PPI.

4. Conclusions

This investigation experimentally studied the convective heat transfer and pressure drop in porous channels with 90-deg turned flow. The heat transfer and pressure drop in straight porous channels were also measured for comparison. Aluminum foams with a porosity of 0.93 were employed. The coolant was air. The size ($W \times H \times L = 60 \times 25.4 \times 60$ mm) of the aluminum foams was fixed. The variable parameters were the ratio of the entry width to the porous sink height (W_j/H), the pore density of the aluminum foam (PPI, pore per inch) and the Reynolds number (Re). In this work, W_j/H is varied from 0.164 to 0.972; PPI are 10 and 40, and Re varies from 1376 to 23,619. The findings of this work support the following conclusions:

(1) For the porous channels with 90-deg turned flow, the θ_w at the corner under the perpendicular flow entry was maximal, declining along the channel axis until x/H was around 1.0, finally approaching a constant value. Therefore, such a configuration should not

be applied to a system with a large heat flux at the channel inlet. Parametric studies have demonstrated that increasing Re increases $\overline{Nu}$ and that the effects of PPI and W_j/H on $\overline{Nu}$ are negligible.

(2) Over range of Re values considered herein, $\overline{Nu}$ in the straight flow configuration was close to the value of the configuration in which the flow turned through 90-deg. However, when $Re < 1000$, $\overline{Nu}$ in the configuration in which the flow turned through 90-deg slightly exceeded that in the straight flow configuration. As $Re > 1000$, $\overline{Nu}$ in the straight flow configuration slightly exceeded $\overline{Nu}$ in the configuration in which flow turned through 90-deg.

(3) For porous channels in which flow turned through 90-deg, the friction factor generally fell as the Reynolds number increased, PPI decreased or W_j/H increased. The friction factor of the straight porous channel was generally lower than that of the porous channel in which flow turned through 90-deg.

(4) Under a particular pumping power constraint ($C_f Re^3$), the $\overline{Nu}$ in the configuration in which the flow turned through 90-deg slightly exceeded that in the straight flow configuration when $C_f Re^3 < 1000$. However, as $C_f Re^3 > 1000$, $\overline{Nu}$ associated with the straight flow configuration slightly exceeded $\overline{Nu}$ in the configuration in which the flow turned through 90-deg. In the latter configuration, increasing W_j/H or reducing PPI slightly increased $\overline{Nu}$ at a given pumping power.

Acknowledgements

The authors would like to thank the National Science Council of the Republic of China for financially supporting this research under Contract No. NSC 92-2622-E-270-003-CC3 and NSC 92-2212-E-344-005.

References

[1] M.L. Hunt, C.L. Tien, Effects of thermal dispersion on forced convection in fibrous media, Int. J. Heat Mass Transfer 31 (1988) 301–309.

[2] F.C. Chou, W.Y. Lien, S.H. Lin, Analysis and experiment of non-Darcian convection in horizontal square packed-sphere channels—1. Forced convection, Int. J. Heat Mass Transfer 35 (1992) 195–205.

[3] G.J. Hwang, C.H. Chao, Heat transfer measurement and analysis for sintered porous channels, ASME J. Heat Transfer 116 (1994) 456–464.

[4] V.V. Calmidi, R.L. Mahajan, Forced convection in high porosity metal foams, ASME J. Heat Transfer 122 (2000) 557–565.

[5] S.Y. Kim, B.H. Kang, J.H. Kim, Forced convection from aluminum foam materials in an asymmetrically heated channel, Int. J. Heat Mass Transfer 44 (2001) 1451–1454.

[6] K. Boomsma, D. Poulikakos, F. Zwick, Metal foams as compact high performance heat exchangers, Mech. Mater. 35 (2003) 1161–1176.

[7] H.L. Fu, K.C. Leong, X.Y. Huang, C.Y. Liu, An experimental study of heat transfer of a porous channel subjected to oscillating flow, ASME J. Heat Transfer 123 (2001) 162–170.

[8] K.C. Leong, L.W. Jin, Heat transfer of oscillating and steady flows in a channel filled with porous media, Int. Commun. Heat Mass Transfer 31 (2004) 63–72.

[9] K.C. Leong, L.W. Jin, An experimental study of heat transfer in oscillating flow through a channel filled with an aluminum foam, Int. J. Heat Mass Transfer 48 (2005) 243–253.

[10] A. Bhattacharya, R.L. Mahajan, Finned metal foam heat sinks for electronics cooling in forced convection, ASME J. Electron. Packag. 124 (2002) 155–163.

[11] K.-H. Ko, N.K. Anand, Use of porous baffles to enhance heat transfer in a rectangular channel, Int. J. Heat Mass Transfer 46 (2003) 4191–4199.

[12] P.X. Jiang, M. Li, T.J. Lu, L. Yu, Z.P. Ren, Experimental research on convection heat transfer in sintered porous plate channels, Int. J. Heat Mass Transfer 47 (2004) 2085–2096.

[13] M.K. Chyu, Y. Hsing, V. Natarajan, J.S. Chiou, Effects of perpendicular flow entry on convective heat/mass transfer from pin-fin arrays, ASME J. Heat Transfer 121 (1999) 668–674.

[14] J.J. Hwang, C.C. Lui, Detailed heat transfer characteristic comparison in straight and 90-deg turned trapezoidal ducts with pin-fin arrays, Int. J. Heat Mass Transfer 42 (1999) 4005–4016.

[15] W.S. Fu, H.C. Huang, Thermal performances of different shape porous blocks under an impinging jet, Int. J. Heat Mass Transfer 40 (1997) 2261–2272.

[16] V.V. Calmidi, R.L. Mahajan, The effective thermal conductivity of high porosity fibrous metal foams, ASME J. Heat Transfer 121 (1999) 466–471.

[17] S.J. Kline, F.A. Mcclintock, Describing uncertainties in single-sample experiments, Mech. Eng. (1953) 3–8.

[18] R.J. Moffat, Contributions to the theory of single-sample uncertainty analysis, ASME J. Fluids Eng. 104 (1986) 250–260.